



Monomeric asymmetric two- and three-cationic monomethine cyanine dyes as novel photoinitiators for free-radical polymerization

Janina Kabatc*, Jerzy Pączkowski

University of Technology and Life Sciences, Faculty of Chemical Technology and Engineering, Seminaryjna 3, 85-326 Bydgoszcz, Poland

ARTICLE INFO

Article history:

Received 9 September 2009

Received in revised form

4 December 2009

Accepted 7 December 2009

Available online 4 January 2010

Keywords:

Photoinitiator

Photopolymerization

Monomethine dyes

ABSTRACT

Several two- and three-cationic monomethine cyanine dyes, possessing a benzothiazolium moiety were synthesized and evaluated as initiators of the free radical polymerization of 2-ethyl-2-(hydroxymethyl)-1,3-propanediol triacrylate under visible light. Dyes bearing 1-methylpyrrolidinium, 4-methylmorpholinium, pyridinium and 3-(N,N-dimethylamino)propan-1-ol substituents were useful initiators. All derivatives absorbed in the region 510–570 nm and displayed molar absorption coefficients of 40 000–60 000 dm³ mol^{−1} cm^{−1}. A kinetic study of photoinitiated polymerization performed with the use of the electron donor *n*-butyltriphenylborate salt showed that the dyes were efficient two-component photoinitiators.

Crown Copyright © 2010 Published by Elsevier Ltd. All rights reserved.

1. Introduction

Photopolymerization offers many advantages, such as temporal and spatial control, cost efficiency and solvent-free systems, over traditional, thermally-initiated polymerization. Photopolymerization can be classified by the type of active centre used to initiate the chain reaction of polymerization; free radical photopolymerization is highly prevalent and offers several advantages including wide monomer availability, relatively high reaction rates, and moisture insensitivity. However, free radical photopolymerization also displays serious disadvantages, such as oxygen inhibition and relatively high polymerization shrinkage.

In most cases, the photoinitiation step of a photopolymerization reaction requires the presence of a molecule (photoinitiator, PI), which absorbs the exciting light and leads to radical or cationic or anionic species, through processes which occur in its excited states. Extension of the spectral sensitivity of a photoinitiator can be achieved by adding a photosensitizer (PS) which will absorb the light and then transfer the energy to PI. The development of such multi-component photoinitiating systems PIS (containing PI, PS and optional additives) is very often a way to polymerize pigmented media or to use visible lights.

Radical photoinitiators are very well known to work through cleavage (e.g. at the α or β position of a carbonyl group), electron-

transfer process or H-abstraction (with a hydrogen donor DH). Visible photosensitizers (mostly referred as dyes) are attractive systems either for a direct initiation through visible lights (conventional lamps or laser beams or even sun) or to increase the energy dose received by a substrate irradiated by a polychromatic light [1].

The efficient photosensitive systems for visible-laser induced polymerization reactions are of great practical use in the laser imaging area such as high speed photopolymers in computer-to-plate laser imaging systems, and the data storage area such as holographic recording systems. Many attempts have been made to develop efficient photoinitiating polymerization systems that can be used upon visible light excitation. In these systems, the photo-physical energy transfer from the excited state of the dye to the second component that is supposed to yield a free radical is generally not favored in view of energetic relationship between the dye and the initiating part. Instead of the energy transfer process, a photoinduced electron-transfer process plays an important role in such systems. This process involves the use of a light to initiate electron transfer from a donor to an acceptor molecule. Electron transfer processes in photopolymerization and imaging processes have been reviewed many authors [2–4].

It is generally accepted that the rate of electron-transfer process depends not only on the free energy change but also on the distance between donor and acceptor.

In the classical Marcus theory, the activation energy related to electron-transfer reaction, ΔG_{el}^\ddagger , as it is shown in Eq. (1), is a function of two parameters.

* Corresponding author. Tel.: +48 52 374 9064; fax: +48 52 374 9009.

E-mail address: nina@utp.edu.pl (J. Kabatc).

$$\Delta G_{el}^{\#} = \frac{\lambda}{4} \left(\frac{\lambda + \Delta G_{el}}{\lambda} \right)^2 \quad (1)$$

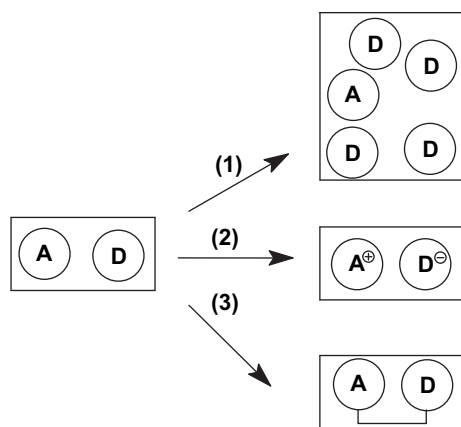
The first one is the free energy change for electron-transfer reaction (ΔG_{el}) and second is the reorganization energy related to the entire nuclear reorganization of the electron-transfer reaction (λ), involving (being the sum) both the geometry change of the reactants (λ_i), and a reorientation of surrounding solvent molecules (λ_s) [5]. λ_s measures the energy change as the solvent dipoles change, and for spherical molecules this change can be expressed by Eq. (2) first used by Marcus.

$$\lambda_s = \Delta e^2 \left(\frac{1}{2r_D} + \frac{1}{2r_A} - \frac{1}{d_{DA}} \right) \left(\frac{1}{\epsilon} - \frac{1}{n^2} \right) \quad (2)$$

where e , ϵ and n have the conventional meaning, r_D and r_A are the radius of donor and acceptor molecules respectively and d_{DA} is the distance separating donor and acceptor. From both equations it is clear that the rate of the electron-transfer reaction depends on the distance separating donor and acceptor in a complex fashion. However, it is visible that the activation energy of ET reaction decreases as distance separating donor and acceptor is increasing, namely, the rate of the ET reaction is higher when the distance separating donor and acceptor is lower. The good illustration of this specific relationship are the results published by Oevering and co-workers, who demonstrated that in their bridged donor-acceptor molecules, the increase of donor-acceptor centre-to-centre separation from 11.5 Å to 13.5 Å decreases the rate of electron-transfer reaction about 10 times [6].

Hence, it is concluded that controlling a donor-acceptor distance is one of the determining factor for the rate of electron-transfer reaction, and with those points in mind, it is necessary to design photoinitiation system where high sensitivity is an indispensable prerequisite. There are three ways, as it is shown in Scheme 1, allowing a decrease of the donor-acceptor distance [7].

The most common and simplest way is the concentration increase of an electron donor (co-initiator). Generally, the average distance (R_0) separating molecules in solution is proportional to the cubic root of molecules concentrations ($R_0 \propto [C]^{1/3}$) [6]. The second way applies an electrostatic interaction between donor and acceptor electrostatic counter-partners. Gottschalk and co-workers reported dye-borate photoinitiating systems in which cationic cyanine dye sensitizer and anionic borate co-initiator are close together in non-polar medium, thus performing higher photosensitivity [7–9]. The third way is to link a donor and acceptor by

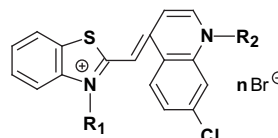


Scheme 1. Three possible ways of decreasing the distance between donor and acceptor in photoinitiating system: (1) increase of concentration, (2) linkage by an ionic interaction, (3) linkage by a covalent bond.

a covalent bond. Dye-linked photoinitiators, in which a radical generating part is brought close to a photosensitizing dye-chromophore by a covalent bond, have been shown to be very useful as free-radical sources [7].

The combination of the first and second ways of increasing of co-initiator concentration on the rate of electron-transfer process and its influence on the rate of free radical polymerization photo-initiated by photoredox pairs (dye/borate) are presented in this paper.

It is our intention to present here the study on photoinitiation abilities of the multi-cationic monomethine dyes **SCH** (structure below) in the presence of borate anion being the electron donor.



The main difference between presented in this paper multi-cationic hemicyanine dyes and described in our previous paper comes from their chemical structure. The introduction more than one organic cation in the hemicyanine dye structure increases of the concentration of a co-initiator in the close proximity of the absorbing chromophore. Thus, the electron-transfer process becomes more efficient results in the better photoinitiating ability of the photoinitiating systems studied.

2. Experimental

2.1. Materials

Substrates for synthesis of the two- and three-cationic monomethine dyes were purchased from Aldrich and POCh (Gliwice, Poland) and were used without further purification. *n*-Butyltriphenylborate tetramethylammonium salt (**B2**) was used as a co-initiator. 2-Ethyl-2-(hydroxymethyl)-1,3-propanediol triacrylate (TMPTA) and 1-methyl-2-pyrrolidinone (MP) were purchased from Aldrich and were used as monomer and solvent, respectively.

2.2. Techniques

- (i) The synthesis of the two- and three-cationic monomethine cyanine dyes was carried out based on the methods described by Deligeorgiev [10,11]. *n*-Butyltriphenylborate tetramethylammonium salt (**B2**) was synthesized based on the method described by Damico [12]. All final products were identified by ^1H NMR spectroscopy. The spectra obtained were the evidence that the reaction products were of the desired structures. The purity of synthesized compounds was determined using thin layer chromatography and by measuring of the melting points. The purity of the dyes was as it is required for spectroscopic studies.
- (ii) Spectroscopic measurements: UV–vis absorption spectra: obtained using Shimadzu UV–vis Multispec – 1500 Spectrophotometer, and steady-state fluorescence: using a Hitachi F-4500 Spectrofluorimeter.
- (iii) The reduction and oxidation potentials of dyes were measured by cyclic voltammetry. An Electroanalytical MTM System model EA9C-4z (Cracow, Poland), equipped with a small-volume cell was used for the measurements. A 1 mm platinum electrode was used as the working electrode. A Pt wire constituted the counter electrode, and an Ag–AgCl electrode served as the reference electrode. The supporting electrolyte was 0.1 M

tetrabutylammonium perchlorate in dry acetonitrile. The solution was deoxygenated by bubbling argon gas through the solution. The potential was swept from -1.6 to 1.6 V with the sweep rate of 500 mV/s to record the current–voltage curve. The dye concentration was 1×10^{-3} M. The average experimental error was ± 0.05 eV.

- (iv) The kinetics of free radical polymerization were studied using a polymerization solution composed of 1 mL of 1-methyl-2-pyrrolidinone (MP) and 9 mL of 2-ethyl-2-(hydroxymethyl)-1,3-propanediol triacrylate (TMPTA). The cyanine borate (photoinitiator) concentration was 1.0×10^{-3} M. A reference formulation contained monomethine cyanine iodide or bromide (dye without an electron donor) instead of cyanine borate salt (photoinitiator). The measurements were carried out at an ambient temperature and the polymerizing mixture was not deaerated before curing.

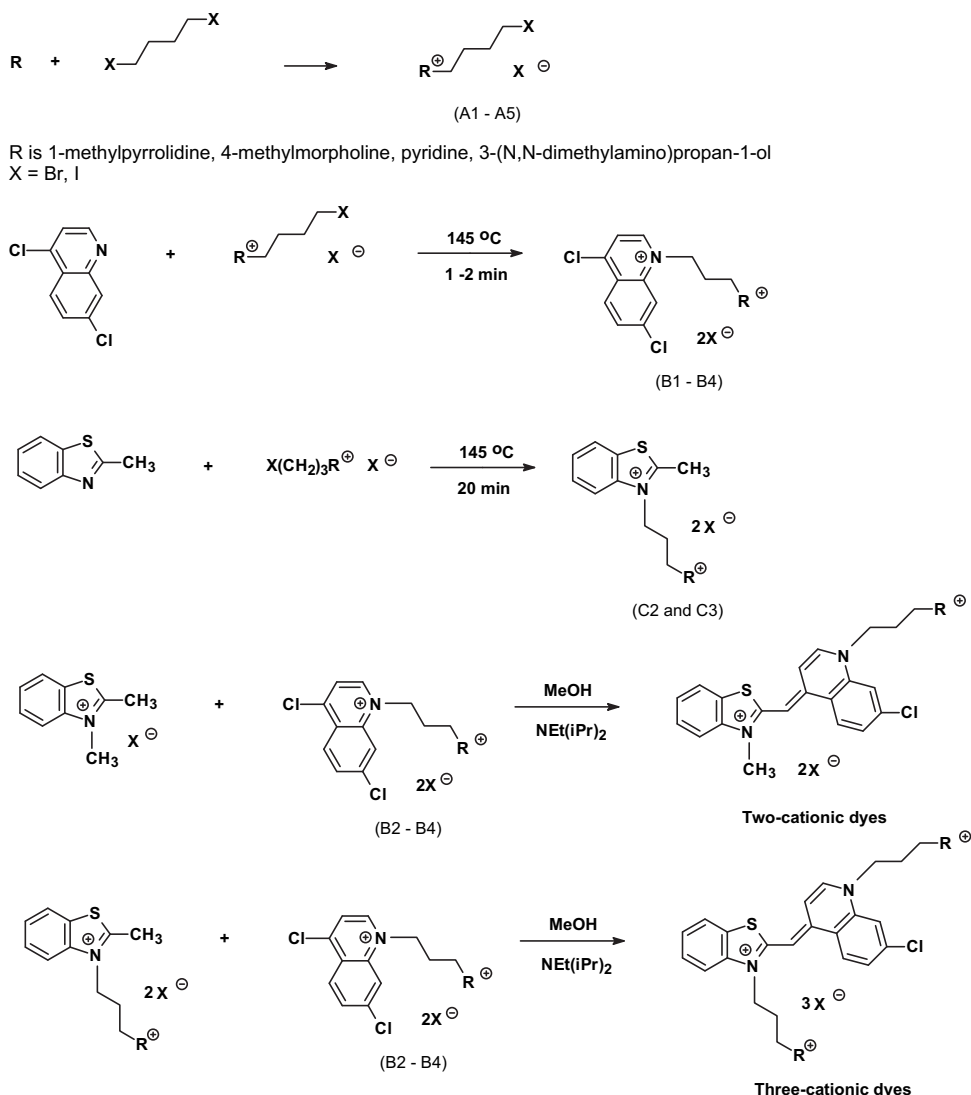
The kinetics of free radical polymerization were measured based on the measurements of the rate of the heat evolution during polymerization in thin film cured sample ($m = 0.035 \pm 0.002$ g). The measurements were performed by measuring photopolymerization exotherms using photo-DSC apparatus constructed on the basis of a TA Instruments DSC 2010 Differential Scanning

Calorimeter. Irradiation of the polymerization mixture was carried out using the emission (line at 514 nm) of an argon ion laser Model Melles Griot 43 series with intensity of light of 20 mW/ 0.196 cm². The light intensity was measured by a Coherent Model Fieldmaster power meter.

The rate of polymerization (R_p) as the number of the total quantity of the functional group, which undergoes reaction per 1 s, was calculated using the formula (1) where dH/dt is maximal heat flow during reaction, M is the molar mass of the monomer, m is the mass of the sample (0.03 g), n is the number of double bonds per monomer molecule and $\Delta H_p^{\text{theor}}$ is the theoretical enthalpy for complete conversion of acrylates' double bonds. $\Delta H_p^{\text{theor}} = 78.2$ kJ/mol for acrylic double bonds [13].

$$R_p = \left(\frac{dH}{dt} \right) \frac{M}{n \Delta H_p^{\text{theor}} m} \quad (3)$$

- (v) The fluorescence measurements were performed at an ambient temperature. The fluorescence lifetimes were measured using an Edinburgh Instruments single-photon counting system (FLS920P Spectrometers). The apparatus



Scheme 2.

utilizes for the excitation a picosecond diode laser generating pulses of about 55 ps at 465 nm. Short laser pulses in combination with a fast microchannel plate photodetector and ultrafast electronics make a successful analysis of fluorescence decay signals with resolution in the range of single picoseconds possible. The dyes were studied at concentration able to provide equivalent absorbance at 465 nm (0.2–0.3 in the 10 mm cell) to be obtained.

2.3. Synthesis

The synthetic approaches that have been applied are outlined below and are based on a condensation reaction of the appropriate quaternary salts of 2-methylbenzothiazolium with quaternized 4,7-dichloroquinoline in the presence of triethylamine [10].

A general route for the synthesis of multi-cationic monomethine cyanine dyes is shown in Scheme 2.

2.3.1. Synthesis of compounds **A1**–**A5**

The appropriate nitrogen-containing base (1-methylpyrrolidine, 4-methylmorpholine, pyridine and 3-(N,N-dimethylamino)propan-1-ol) (0.01 mol), 0.04 mol 1,3-dibromopropane or 1,3-diiodopropane and 30 mL of acetone were mixed in reaction vessel and vigorously stirred for 20 min. The reaction mixture was left for 7 days at room temperature in the dark, after which time, the ensuing precipitate was filtered and air dried [10].

2.3.2. Synthesis of compounds **B1**–**B4**

Intermediates **A1**–**A5** (0.01 mol) and 0.015 mol 4,7-dichloroquinoline were mixed and heated together in a reaction vessel at 140–145 °C for 30 s. After cooling to a room temperature 30 mL of acetone was added. The resulting precipitate was filtered and dried in a desiccator.

2.3.3. Synthesis of compounds **C2** and **C3**

2-Methylbenzothiazole (0.015 mol) and 0.01 mol **A1** or **A4** were mixed and heated at 140–145 °C for 20 min. After cooling to room temperature, 30 mL of acetone was added. The ensuing precipitate was filtered and air dried.

2.3.4. Synthesis of two- and three-cationic dyes

Intermediates **C1**, **C2** or **C3** (0.002 mol) and 0.0022 mol **B1**–**B4** were ground together and suspended in 15 mL of methanol. N-Ethyl-diisopropylamine (0.004 mol) was added dropwise during 1–2 min and the reaction mixture was vigorously stirred at room temperature for 2 h. The resulting red precipitate was filtered and air dried. The dyes were twice recrystallized in ethanol.

3. Results and discussion

Thiazole Orange and related dyes can be synthesized according to the method described by Brooker et al. by the reaction of 2-methylthiobenzothiazolium salts with 1-alkyl-4-methylquinolinium salts [10,14,15]. The disadvantage of this method is the evolution of toxic methylmercaptan [10]. To avoid this we used an improved method described by Deligeorgiev [10]. It involved condensation of quaternized 2-chloro-heterocycles with quaternized 2- or 4-methyl-heterocyclic compounds in the presence of a basic agent as triethylamine.

The dye synthesis requires some intermediates to be prepared. Thus, 1-methylpyrrolidine, 4-methylmorpholine, pyridine and 3-(N,N-dimethylamino)propan-1-ol were quaternized with 1,3-dibromopropane and 1,3-diiodopropane giving the quaternary salts **A1**–**A5** (Scheme 2 and Table 1).

In the second step 4,7-dichloroquinoline was quaternized at solvent-free conditions for extremely short reaction time (60 – 120 s) with the quaternary salts **A1**–**A5**, to give intermediates **B1**–**B4** (Scheme 2 and Table 1).

The 2-methylbenzothiazole derivatives **C1**–**C3** were prepared according Deligeorgiev's method [11] by quaternization of 2-methylbenzothiazole with methyl iodide, and the quaternary salts **A1** or **A4** (Scheme 2, Table 1).

The two-cationic (**S0CH4**, **S0CH5**, **S0CH6**) and three-cationic dyes (**S1CH4**, **S1CH5**, **S1CH6**, **S5CH4**, **S5CH5**, **S5CH6**) were synthesized by the condensation of 2-methylbenzothiazolium salts **C1**, **C2**

Table 1
Chemical structures of compounds synthesized.

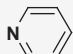
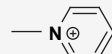
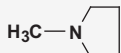
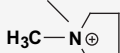
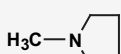
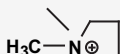
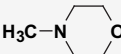
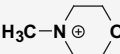
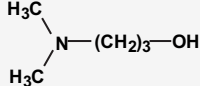
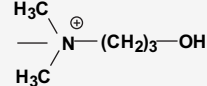
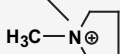
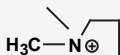
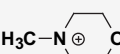
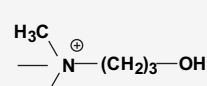
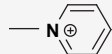
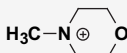
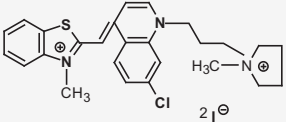
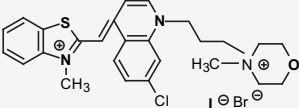
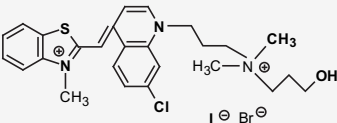
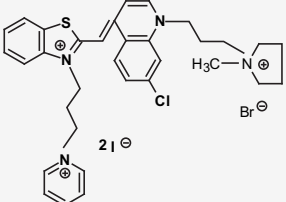
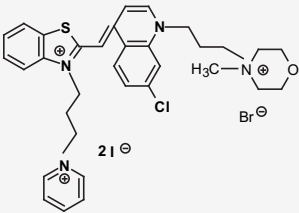
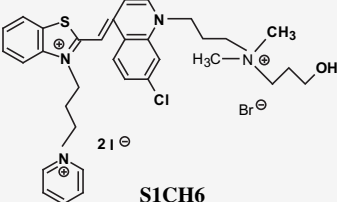
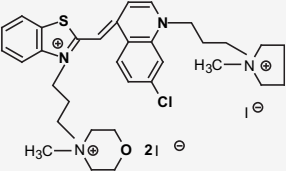
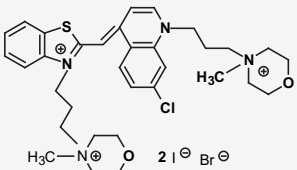
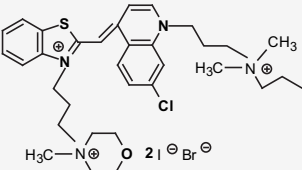
Compound	R	R ⁺	X
A1			I
A2			Br
A3			I
A4			Br
A5			Br
Compound	Substrate	R ⁺	X
B1	A2		Br
B2	A3		I
B3	A4		Br
B4	A5		Br
Compound		R ⁺	X
C2			I
C3			I

Table 2¹H NMR spectra and yields of two-cationic and three-cationic dyes synthesized.

Dye structure	Yield [%]/m.p. [°C]	¹ H NMR (DMSO) δ (ppm)
 <p>S0CH4</p>	62.4/239–44	2.074–2.103 (d) 4H, –CH ₂ –, 2.303 (m) 2H, –CH ₂ –, 3.004 (s) 3H, N ⁺ CH ₃ , 3.451–3.504 (t) 6H, N ⁺ –CH ₂ –, 4.023–4.112 (s) 3H, N ⁺ –CH ₃ , 4.546–4.616 (t) 2H, N–CH ₂ –, 6.949 (s) 1H, –CH=, 7.330–7.367 (t) 1H, Ar, 7.423–7.499 (t) 1H, Ar, 7.607–7.689 (t) 1H, Ar, 7.737–7.870 (m) 2H, Ar, 8.035–8.116 (t) 1H, Ar, 8.273 (s) 1H, Ar, 8.520–8.575 1H, Ar, 8.817–8.863 1H, Ar
 <p>S0CH5</p>	60/233–253	1.233–1.270 (d) 4H, –O–CH ₂ –, 1.682–1.741 (d) 2H, –N–CH ₂ –, 2.072 (d) 2H, –CH ₂ –, 3.459 (s) 6H, N ⁺ –CH ₂ –, 3.808–3.836 3H, N ⁺ –CH ₃ , 3.905–4.015 (s) 3H, N ⁺ –CH ₃ , 6.949 (s) 1H, –CH=, 7.464–7.619 (t) 4H, Ar, 8.055–8.152 (t) 3H, Ar, 8.784 2H, Ar
 <p>S0CH6</p>	57/191–195	1.200–1.276 (t) 2H, –CH ₂ –, 1.928 (m) 4H, –CH ₂ –, 2.072–2.162 (m) 2H, N–CH ₂ –, 3.032 (s) 6H, N ⁺ CH ₃ , 3.700–3.730 (t) 2H, –O–CH ₂ –, 3.982 (s) 3H, N ⁺ CH ₃ , 4.250 (d) 2H, N ⁺ CH ₂ –, 4.568 (d) 2H, N ⁺ CH ₂ –, 6.101–6.143 (d) 1H, –OH, 6.925–6.960 (s) 1H, –CH=, 7.312–7.506 (t) 2H, Ar, 7.585–7.693 1H, Ar, 7.749–7.973 (m) 2H, Ar, 8.011–8.187 (t) 1H, Ar, 8.260 (d) 1H, Ar, 8.528–8.564 (d) 1H, Ar, 8.801–8.865 (2d) 1H, Ar.
 <p>S1CH4</p>	68.65/215–227	1.678 2H, N–CH ₂ –, 2.072 (d) 4H, –CH ₂ –, 2.966–2.997 (m) 2H, –CH ₂ –, 3.019–3.195 (s) 3H, N ⁺ CH ₃ , 3.532–3.807 (t) 6H, N ⁺ –CH ₂ –, 3.953–3.990 (m) 2H, –CH ₂ –, 4.697–4.772 (t) 4H, N ⁺ –CH ₂ –, 6.076–6.143 (d) 2H, Ar, 6.900 (s) 1H, –CH=, 7.310–7.391 (d) 2H, Ar, 7.502–7.541 (d) 1H, Ar, 7.619 (t) 1H, Ar, 7.766–7.775 (d) 2H, Ar, 7.949–8.013 (d) 2H, Ar, 8.048–8.092 (t) 3H, Ar, 9.096–9.123 2H, Ar, 8.817–8.863 1H, Ar
 <p>S1CH5</p>	60/265–270	1.200–1.274 (d) 4H, –O–CH ₂ –, 1.9 (d) 2H, –N–CH ₂ –, 2.076 (d) 4H, –CH ₂ –, 3.451 (s) 6H, N ⁺ –CH ₂ –, 3.570–3.655 (s) 3H, N ⁺ –CH ₃ , 3.834–3.858 (s) 3H, N ⁺ –CH ₃ , 6.704 (s) 1H, –CH=, 6.740–9.050 (t) 10H, Ar
 <p>S1CH6</p>	57/207–210	1.138–1.274 (t) 6H, –CH ₂ –, 1.849–1.928 (m) 2H, –N–CH ₂ –, 3.008–3.213 6H, –N ⁺ CH ₃ , 3.442–3.470 (t) 4H, –N–CH ₂ –, 3.532–3.720 (t) 4H, –N–CH ₂ –, 4.686–4.761 (t) 2H CH ₂ –OH, 7.297–7.337 (s) 1H, –CH=, 7.405–7.444 (d) 1H, Ar, 7.764–7.825 (t) 2H, Ar, 7.916–7.986 1H, Ar, 7.749–7.973 (m) 2H, Ar, 8.172–8.237 (t) 2H, Ar, 8.607–8.639 (d) 1H, Ar, 8.735–8.760 (d) 1H, Ar, 8.857–8.887 (d) 2H, Ar, 9.075–9.108 (d) 2H, Pyr
 <p>S5CH4</p>	69.4/215–219	1.241–1.274 4 H, –CH ₂ –, 2.077–2.106 (d) –CH ₂ –, 2.966–2.997 (m) 2H, –CH ₂ –, 3.007 (s) 3H, N ⁺ CH ₃ , 3.110–3.197 N ⁺ –CH ₂ –, 3.326 (s) 3H, N ⁺ CH ₃ , 3.505–3.626 (t) 4H, –O–CH ₂ –, 3.934–4.157 3H, 4.589–4.619 (d) 4H, N ⁺ –CH ₂ –, 4.769 (t) N–CH ₂ –, 6.952 (s) 1H, –CH=, 7.337–7.370 (d) 2H, Ar, 7.421–7.458 (t) 1H, Ar, 7.652 (t) 1H, Ar, 7.743–7.912 (d) 2H, Ar, 8.084–8.142 (t) 1H, Ar, 8.282–8.329 (d) 1H, Ar, 8.549–8.674 (2d) 1H, Ar, 8.820–8.923 (t) 1H, Ar

(continued on next page)

Table 2 (continued)

Dye structure	Yield [%]/m.p. [°C]	¹ H NMR (DMSO) δ (ppm)
 <p>S5CH5</p>	60/252	1.201–1.274 (d) 8H, –O–CH ₂ –, 1.677 (d) 4H, –N–CH ₂ –, 2.073 (d) 4H, –CH ₂ –, 2.784 3H, N ⁺ –CH ₃ , 3.454 (d) 4H, –O–CH ₂ –, 3.707–3.765 2H, –CH ₂ –OH, 3.930 2H, N ⁺ CH ₂ –, 4.033–4.066 (t) 4H, N ⁺ CH ₂ –, 4.267–4.296 2H, N ⁺ CH ₂ –, 5.900 1H, –OH, 6.910 (s) 1H, –CH=, 7.340–7.443 (t) 1H, Ar (benzothiazole), 7.509–7.842 2H, Ar, 7.930–8.025 (m) 2H, Ar, 8.062–8.142 (t) 2H, Ar, 8.150–8.186 (d) 2H, Ar
 <p>S5CH6</p>	72.35/120–130	1.209–1.282 (t) 2H, –CH ₂ –, 1.941 (m) 4H, –CH ₂ –, 2.183 (m) 2H, N–CH ₂ –, 3.069 (s) 9H, N ⁺ CH ₃ , 3.454 (d) 4H, –O–CH ₂ –, 3.707–3.765 2H, –CH ₂ –OH, 3.930 2H, N ⁺ CH ₂ –, 4.033–4.066 (t) 4H, N ⁺ CH ₂ –, 4.267–4.296 2H, N ⁺ CH ₂ –, 5.900 1H, –OH, 6.910 (s) 1H, –CH=, 7.340–7.443 (t) 1H, Ar (benzothiazole), 7.509–7.842 2H, Ar, 7.930–8.025 (m) 2H, Ar, 8.062–8.142 (t) 2H, Ar, 8.150–8.186 (d) 2H, Ar

or **C3** with 4,7-dichloroquinolinium derivatives **B2–B4** in the presence of the sterically hindered base (N-ethyldiisopropylamine) in mild conditions (room temperature) and for relatively short reaction time (2 h) (Scheme 2).

The multi-cationic dyes were synthesized in yield of about 60–70 % and their structures were confirmed by ¹H NMR spectroscopy (Table 2).

Because of the ionic structure of the dyes investigated, they are poorly soluble in non-polar and medium polarity solvents. From the analysis of the novel photoinitiators structures compiled in Table 2, it is evident that all the dyes under the study possess identical chromophore. Thus, one can anticipate that they should display very similar spectroscopic and photophysical properties.

For the illustration, the electronic absorption (UV–vis) and emission spectra of the selected dye are presented in Figs. 1 and 2.

All tested dyes have one absorption band in the visible region located approximately at 520 nm and strong fluorescence emission

characterized by Stokes shift of about 2000–3000 cm^{−1}. The corresponding molar absorption coefficients are high with values between 40 000–60 000 dm³ mol^{−1} cm^{−1}. The position of the absorption band does not depend on the solvent polarity.

Table 3 summarizes the spectroscopic properties (absorption and fluorescence) of all tested dyes.

The electrochemistry of dyes was investigated in the cathodic region by carrying out cyclic voltammetry experiments using 1 × 10^{−3} M solutions of the relevant compound dissolved in deoxygenated 0.1 M of tetrabutylammonium perchlorate in anhydrous acetonitrile at room temperature. The electrochemical studies (Table 3) showed that tested dyes undergo electrochemical reduction in acetonitrile solution and have reduction potential in the range from −1.40 V to −1.06 V.

The results obtained from electrochemical measurements are surprising. As expected from the chemical structure of dyes tested, similar responses should be observed for all compounds, suggesting the same type of electrochemical behavior characterizing the

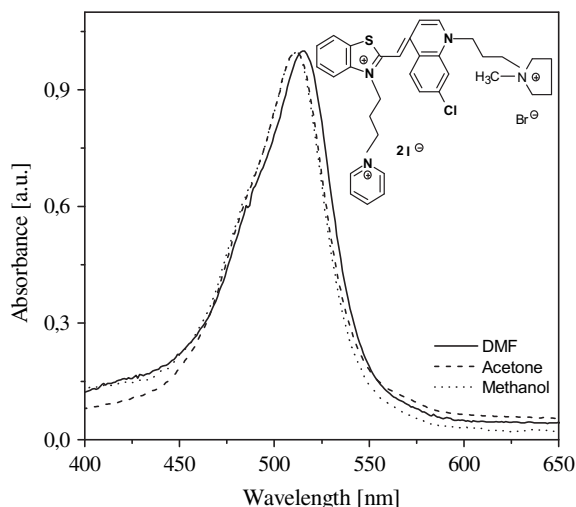


Fig. 1. Electronic absorption spectra of selected monomethine dye N-[(3-pyridin)propyl]-2-methylidene-4-[7-chloro-N-[3-(N-methylpyridinium)propyl]quinolinbenzothiazolium cation (**S1CH4**) in N,N-dimethylformamide, acetone and methanol as a solvent at 293 K (dye marked in the figure).

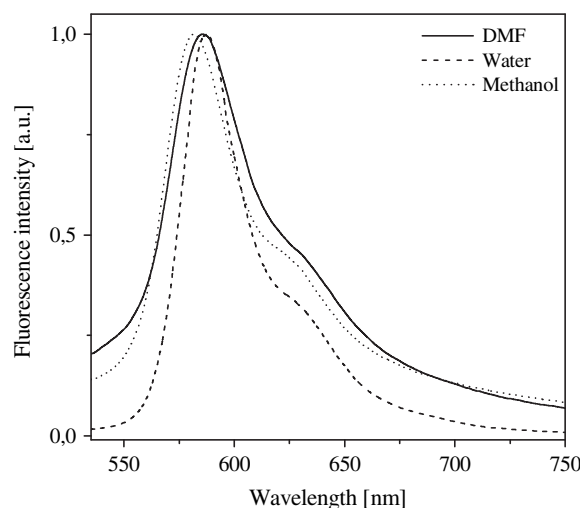


Fig. 2. The emission spectra of N-[(3-pyridin)propyl]-2-methylidene-4-[7-chloro-N-[3-(N,N-dimethylamino)propan-1-olo]propyl]quinolinbenzothiazolium cation (**S1CH6**) in N,N-dimethylformamide, water and methanol as a solvent, respectively.

Table 3
Spectroscopic and electrochemical properties of tested dyes.

Dye	$\lambda_{\max}^{\text{abs}}$ ^a [nm]	$\lambda_{\max}^{\text{abs}}$ ^b [nm]	$\lambda_{\max}^{\text{fl}}$ ^a [nm]	$\lambda_{\max}^{\text{fl}}$ ^b [nm]	E_{red} [eV]	E_{00}^{a} [eV]	E_{00}^{b} [eV]
S0CH4	516	512	576	575	−1.30	2.34	2.36
S0CH5	516	512	582	575	−1.20	2.20	2.21
S0CH6	516	512	574	573	−1.40	2.36	2.38
S1CH4	515	513	583	581	−1.18	2.27	2.35
S1CH5	516	512	585	585	−1.06	2.25	2.31
S1CH6	518	514	587	585	−1.25	2.38	2.37
S5CH4	516	514	582	579	−1.23	2.33	2.33
S5CH5	517	514	583	578	−1.12	2.30	2.2
S5CH6	516	513	581	578	−1.30	2.38	2.37

^a Measured in N,N-dimethylformamide.

^b Measured in methanol.

electro-activity of the whole series. In other words, when one compares the chemical structure of tested dyes, one can see that the structure of chromophore is the same for all tested dyes. Therefore, one can expect that the reduction potential for all dyes should have the same value as measured for mono-cationic parent dye ($R_1 = \text{CH}_3$, $R_2 = -\text{CH}_2\text{CH}_2\text{CH}_2\text{Br}$) and being equal about −1.0 eV. However, the measured reduction potentials are lower. The observed differences between the reduction potential measured for two- and three-cationic monomethine dyes may arise from the differences between the ionic strength of electrolyte (0.1 M tetramethylammonium perchlorate) in proximity to the chromophore caused by the presence of additional quaternary ammonium salt molecules deriving from additional groups of salt that are covalently bonded to the chromophore [16]. The increase of an ionic strength of an electrolyte estimated is about 3% and 6% for two- and three-cationic dyes, respectively. The increase of an ionic strength of an electrolyte causes the decrease of an ion activity coefficient and thus causes a decrease of the reduction potentials of dyes. The influence of the ionic strength observed is not the same for all tested dyes. As can be seen from the values presented in Table 3, the reduction potentials for dyes possessing 3-(N,N-dimethylamino) propan-1-ol group (serie SCH6) are the most negative, implying that the larger amount of energy must be rendered to these dyes in order to reduce them. Comparison of these values with those corresponding to the potentials obtained for other dyes (serie SCH4 and SCH5), suggests that the terminal hydroxylic group in these dyes should be somehow stabilizing the positive charge of the dye moiety. Since the alkyl chain that characterizes the structure of compounds S0CH6, S1CH6 and S5CH6 bears six methylene groups, and the concentration of the electro-active compound in the voltammetric experiments is relatively low, we speculate that there must exist a folded form of those compounds that, by means of an electrostatic interaction, should be responsible for the more negative reduction potential computed from our experimental data. Similar results in electrochemical behavior of stilbazolium dyes were observed by other groups [17,18].

It is necessarily to emphasize that, in order to transfer the multi-cationic monomethine dyes into efficient free radical polymerization initiating system, the exchange of an anion type from iodide or bromide on borate anion was needed. As electron donor for the photoinitiated free radical polymerization *n*-butyltriphenylborate salt was used. The free energy change for the electron transfer (ΔG_{el}) between the excited state of monomethine dye and the borate salt was calculated from Rehm–Weller equation [19] (Eq. (4)):

$$\Delta G_{\text{el}} = E_{\text{ox}}(D^+/D) - E_{\text{red}}(A/A^{\cdot-}) - Z e^2 / \epsilon a - E_{00} \quad (4)$$

in which $E_{\text{ox}}(D^+/D)$ is the oxidation potential of the electron donor molecule (for *n*-butyltriphenylborate anion $E_{\text{ox}} = 1.16$ V), $E_{\text{red}}(A/$

$A^{\cdot-})$ is the reduction potential of electron acceptor (monomethine dye), $Z e^2 / \epsilon a$ is the Coulombic energy, normally considered negligible in high-dielectric solvents, and E_{00} is the singlet energy of the photosensitizer.

The thermodynamic condition for spontaneous electron transfer is that the free energy change ΔG_{el} , expressed by the Rehm–Weller equation should have negative values [19].

The calculated (using the Rehm–Weller equation) thermodynamical properties of new monomethine borate salts are listed in Table 4. For the calculation of ΔG_{el} the energy of the 0,0 transition for the singlet state was taken into account.

It should be noted that according to the Schuster's studies the oxidation potential of tested *n*-butyltriphenylborate salt determined by electrochemical method have only approximate meaning. This is because of a very short lifetime (about 250 fs) of the boranyl radical formed as a result of the photoinduced electron-transfer process [8,9]. The values of ΔG_{el} for tested photoredox pairs oscillate in the range from −0.09 eV to 0.20 eV.

In the next step the polymerization photoinitiation efficiencies of TMPTA/MP mixture were measured for several combinations of dye/borate salt applied as photoinitiating system. Nine monomethine dyes as *n*-butyltriphenylborate salts were used as two-component photoinitiating systems. The general structure of the photoinitiators tested is presented in Chart 1.

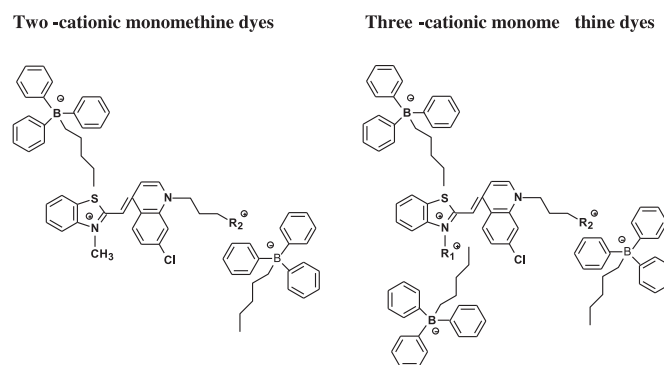


Chart 1.

In order to optimize the polymerization mixture composition, at the beginning, the cyanine borate concentration effect on observed rate of polymerization was determined. In the conventional UV–vis photopolymerization, R_p increases when more initiator is used, however it decreases rapidly if too much initiator is added. This effect is attributed to the “inter filter effect” and becomes more

Table 4

Thermodynamic properties, fluorescence lifetimes, rate constant of electron-transfer process, rates of polymerization and relative rates of photoinitiation abilities of monomethine cyanine borates photoredox pairs.

Dye	ΔG_{el} [eV]		$\tau_{\text{fl } 1}$ [ns]	$\tau_{\text{fl } 2}$ [ns]	$\tau_{\text{fl } 3}$ [ns]	R_p [$\mu\text{mol/s}$]	$1 + \ln R_p$ [a.u.]
	DMF	MeOH					
S0CH4	0.12	0.10	0.30	0.76	5.59	1.26	2.99
S0CH5	0.16	0.15		2.14	6.84	0.872	2.61
S0CH6	0.20	0.18	0.23	2.20	7.24	0.696	2.398
S1CH4	0.07	0.09	0.39	2.47	7.52	0.171	1
S1CH5	−0.03	−0.09	0.93	3.78	8.43	1.628	3.247
S1CH6	0.03	0.06	0.31	1.35	4.89	0	—
S5CH4	0.06	0.06	0.53	3.01	8.41	1.048	2.807
S5CH5	−0.02	0.08	0.57	3.12	7.91	0.619	2.281
S5CH6	0.08	0.09	0.83	3.36	8.78	0.874	2.626

k_{el} calculated for the conformer possessing about 70% percentage participation.

significant for photoinitiators with high molar extinction coefficient (for tested monomethine borate salt ϵ is about $4 \times 10^4 \text{ M}^{-1} \text{ cm}^{-1}$). Fig. 3 presents the relationship between the initial rate of polymerization (taken as the slope of linear part of kinetic curve at its initial time) and concentration of photoinitiator.

It is evident that as the photoinitiator concentration is increasing, the initial rate of polymerization increases and reaches a maximum followed by a continuous mild decrease. For the tested photoinitiators under irradiation conditions the highest rate of polymerization was observed at the photoinitiator (monomethine *n*-butyltriphenylborate salt) concentration of about $1 \times 10^{-3} \text{ M}$.

The kinetic curves obtained for the photoinitiated polymerization of TMPTA/MP (9:1) mixture recorded for selected two- and three-cationic monomethine borate salts, under irradiation with a visible light, are shown in Figs. 4 and 5 for illustration.

Additionally, from Figs. 4 and 5 and measured rates of free radical polymerization (Table 4) it is evident that the efficiency of polymerization depends on the dye structure. It is apparent that the three-cationic dyes possessing N-methylmorpholinium group attached to the benzothiazole moiety are the most effective initiating photoredox pairs. The kinetic curves obtained during the free radical polymerization of the TMPTA/MP polymerizing mixture initiated by the well known two-component photoinitiating system composed of Rose Bengal derivative (RBAX) and N-phenylglycine is also presented for comparison (Fig. 6).

The detailed revision of the data presented in Table 4 suggests that the rate of polymerization might be a function of the rate of primary process, e.g. the rate of electron transfer within the photoredox pair. Taking into consideration the Marcus theory, the rate of free radical polymerization photoinitiated by monomethine cyanine borate salts can be expressed by following equation [20–22]:

$$R_p = -\frac{d[M]}{dt} = k_p[M] \sqrt{\frac{I_a \chi Z \exp\left[-(\lambda + \Delta G_{el})^2 / 4\lambda RT\right]}{k_t}} \quad (5)$$

where χ – transmission coefficient, Z – universal frequency factor ($6 \times 10^{12} \text{ s}^{-1}$) at 25 °C, λ – total reorganization energy, ΔG_{el} – free energy of the electron-transfer process, described by earlier mentioned Rehm–Weller equation (eq. (4)).

The rate of free radical polymerization can also be described in the simpler logarithmic form:

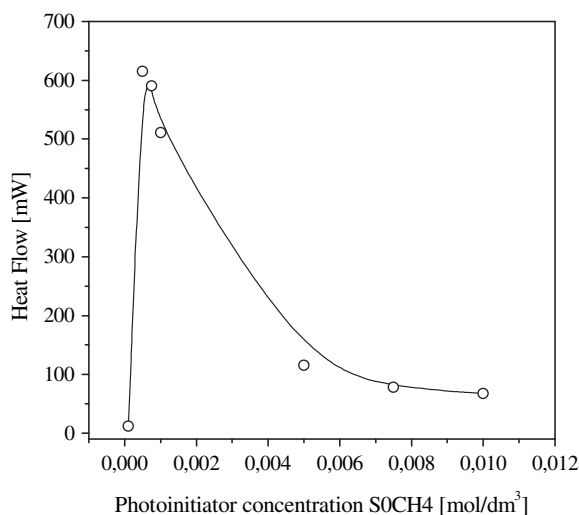


Fig. 3. Rate of polymerization versus monomethine borate **S0CH4B2** concentration.

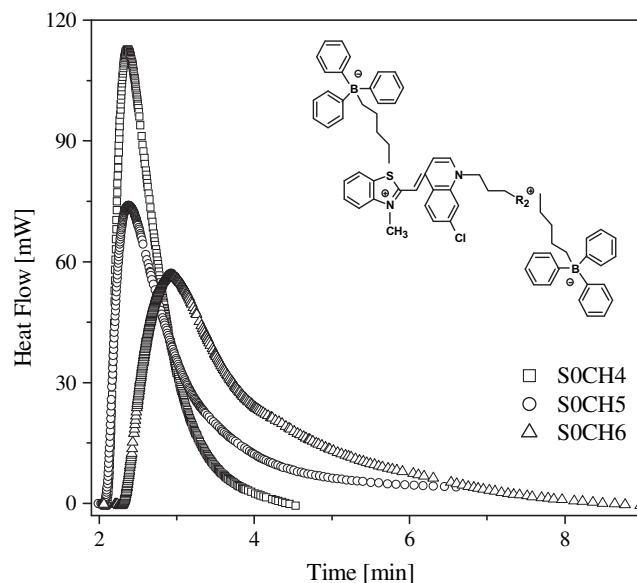


Fig. 4. Family of kinetic curves recorded during the measurements of the flow of heat emitted during the photoinitiated polymerization of the TMPTA/MP (9/1) mixture initiated by two-cationic monomethine borates marked in the figure. The dye photoinitiator concentration was $1 \times 10^{-3} \text{ M}$, $I_a = 20 \text{ mW}/0.196 \text{ cm}^{-1}$. The applied dyes possessed various chromophores and identical borate.

$$\ln R_p = A - (\lambda + \Delta G_{el})^2 / 8\lambda RT \quad (6)$$

where A for initial time of polymerization is the sum: $\ln k_p - 0.5 k_t + 1.5 \ln[M] + 0.5 \ln I_a$ (here k_p , k_t denote the rate constant of polymerization and termination, respectively, $[M]$ is the monomer concentration, I_a is the intensity of absorbed light), λ is the reorganization energy necessary to reach the transitions states both of excited molecule and solvent molecules.

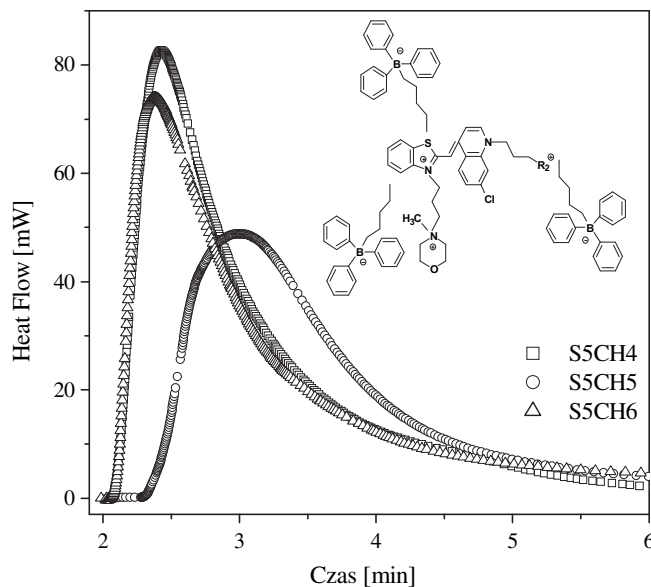


Fig. 5. Family of kinetic curves recorded during the measurements of the flow of heat emitted during the photoinitiated polymerization of the TMPTA/MP (9/1) mixture initiated by three-cationic monomethine borates marked in the figure. The dye photoinitiator concentration was $1 \times 10^{-3} \text{ M}$, $I_a = 20 \text{ mW}/0.196 \text{ cm}^{-1}$. The applied dyes possessed various chromophores and identical borate.

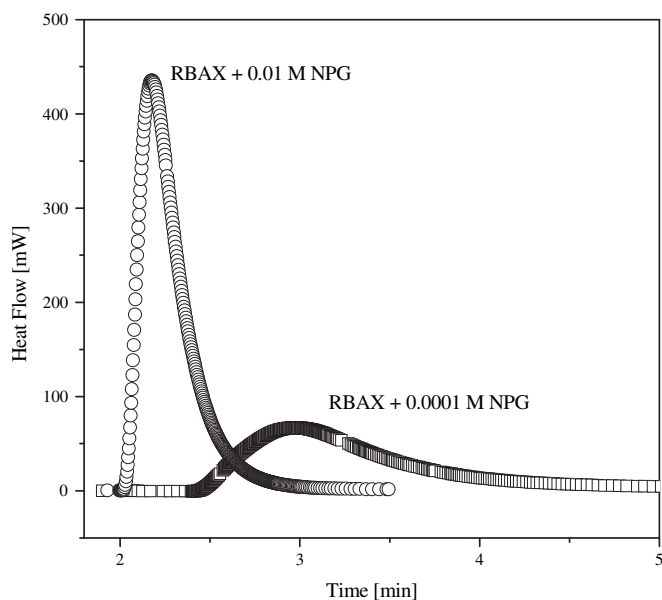


Fig. 6. Family of kinetic curves recorded during the measurements of the flow of heat emitted during the photoinitiated polymerization of the TMPTA/MP (9/1) mixture initiated by two-component photoinitiating system composed of Rose bengal derivative (RBAX) and N-phenylglycine (NPG). The concentration of both components is marked in the figure, $I_a = 20 \text{ mW}/0.196 \text{ cm}^{-1}$.

Eq. (6) clearly indicates that, if the rate of electron-transfer process controls the observed rate of photopolymerization, one should observe a parabolic (or a part of parabola) relationship between the logarithm of polymerization rate and the free energy change ΔG_{el} .

Fig. 7 presents the relationship between the normal logarithm of the TMPTA polymerization rate as a function of the ΔG_{el} for the initiating systems, possessing the same chromophores and different organic cations attached to the heterocyclic rings (Table 2).

Obtained relationships are roughly linear for all dyes triplets possessing identical organic cations attached to benzothiazole nitrogen atom and different organic cations attached by an alkyl chain to quinolinium nitrogen atom. Similar slopes and y-intercepts observed derive probably from similar dissociation degrees of ammonium borate salts that are covalently attached to the dye-chromophore.

In order to explain, the influence of the primary process, e.g. electron-transfer process on the rate of free radical polymerization the kinetics of quenching of the excited singlet state was studied using the measurements of the fluorescence lifetime of tested dyes, namely the dyes with bromide, iodide and dyes in the presence of *n*-butyltriphenylborate anion as a counter-ion. The examples of the fluorescence decay curves are shown in Fig. 8.

The effect of bromide or iodide anion exchange to *n*-butyltriphenylborate anion is shown in Fig. 8. From the inspection data presented in Table 4 it is clearly seen that borate anion strongly decreases monomethine cyanine dye fluorescence lifetime and this, in turn, suggest that borate ion quenches the excited state of monomethine cyanine dye. The results obtained during fluorescence lifetime measurements show the multiexponential fluorescence decay. The shortest lifetime observed was about 0.5 ns and the longest lifetime oscillated from 6 to 9 ns. The percentage participation of conformer possessing the shortest lifetimes is about 5–10%.

As it was mentioned above, the electron-transfer process between the cyanine and borate ions causes the quenching and

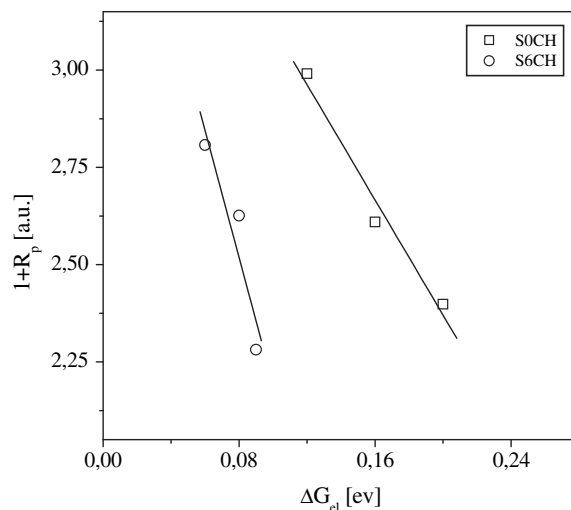


Fig. 7. The dependence of the rate of photoinitiated polymerization on the free energy (ΔG_{el}) for the photoinduced electron-transfer process from borate anion to the excited state of two- and three-cationic cyanine dye, possessing the same chromophores and different organic group attached to the nitrogen atom of quinolinium ring. The free energy of activation of electron-transfer process used for graph drawing is the averaged value obtained for all ΔG_{el} established for three series of the dyes.

simultaneous shortening of the fluorescence lifetime of monomethine chromophore tested.

The results obtained from fluorescence lifetime quenching experiments were analyzed with the use of the Stern–Volmer relationship (Eq. (7)):

$$\frac{\tau_0}{\tau} = 1 + K_q[Q] = 1 + k_q\tau[Q] \quad (7)$$

where τ_0 and τ are the fluorescence lifetimes of the tested dyes in the absence and presence of quencher, respectively; K_q is the Stern–Volmer constant, k_q is the quenching constant. From the known fluorescence lifetime τ and from the slope of the linear

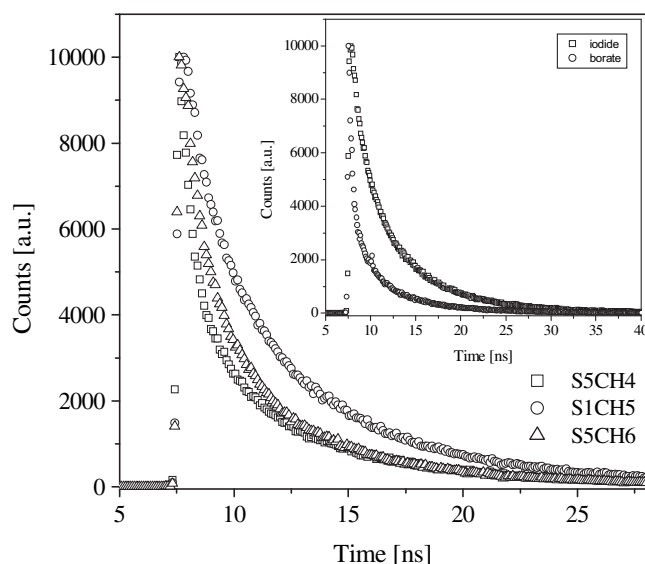


Fig. 8. The influence of the monomethine cyanine dye structure of the fluorescence lifetime of the excited singlet state. Fluorescence measurements performed in MP-ethyl acetate (4:1) solution. Inset: The influence of borate anion on the fluorescence decay of S1CH4.

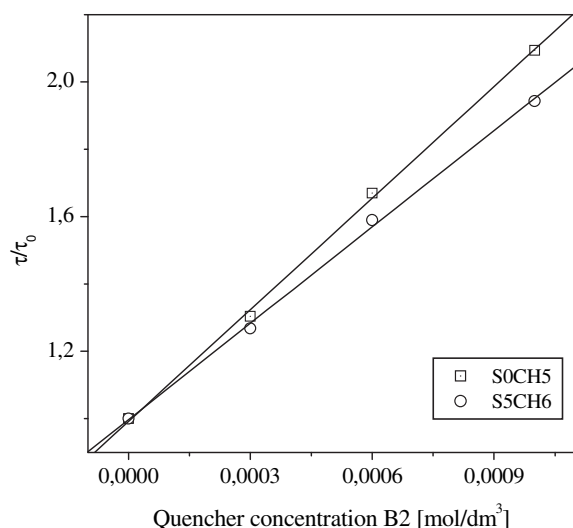


Fig. 9. Stern–Volmer plot for quenching of fluorescence of two- and three-cationic monomethine dyes **SCH** by tetramethylammonium *n*-butyltriphenylborate (**B2**) in ethyl acetate – MP (20:1) solution based on fluorescence lifetimes measurements, respectively. Measurements were performed for the main component of the fluorescence decay (more than 70%).

relationship of Stern–Volmer plot (Fig. 9), one can calculate the k_q value.

The quenching rate constants (k_q) for the photoinduced electron-transfer reaction between the singlet state of monomethine cations and the butyltriphenylborate anion are collected in Table 4.

The quenching rate constants (k_q) are equal about $1 \times 10^{11} \text{ M}^{-1} \text{ s}^{-1}$. The rate constants obtained for dye-borate ion pairs are higher than those commonly observed for intermolecular electron-transfer reactions since ion pairing eliminates the limitation caused by diffusion. This is the evidence that the reaction of electron transfer occurs mostly in an intra-ion-pair assembly. Similar observation for other cyanine dyes is described by Schuster et al. [8,9].

4. Conclusions

Nine multi-cationic monomethine cyanine dyes, based on the Thiazole Orange chromophore were synthesized. The corresponding molar absorption coefficients at 520 nm oscillates between

40 000 and $60\,000 \text{ dm}^3 \text{ mol}^{-1} \text{ cm}^{-1}$. The multi-cationic monomethine dyes are good photoinitiators of free radical polymerization in presence of the effective electron donor such as *n*-butyltriphenylborate salt. Their photoinitiating ability depends on the chemical structure of the dye. Because of the same chromophore structure in all sensitizers tested, the photoinitiating abilities of the photoinitiating systems under study are similar. The type of a substituent at the nitrogen atom in the benzothiazole moiety does not have significant effect on photoinitiating ability. They participate in the photoreducible sensitization of the photoinitiated polymerization.

Acknowledgment

This work was supported by The Ministry of Science and Higher Education (MNiSW) (grant no N N204 219734).

References

- [1] Fouassier JP. In: Fouassier JP, editor. Photochemistry and UV curing: new trends, vol. 1. India: Research Signpost; 2006. p. 3–4.
- [2] Fouassier JP. Recent Res Develop Polymer Sci 2000;4:131.
- [3] Monroe BM, Weed GC. Chem Rev 1993;93:435.
- [4] Eaton DF. Adv Photochem 1985;13:427.
- [5] Turro NJ. Modern molecular photochemistry. California: The Benjamin/Cummings Publishing; 1978. p. 316.
- [6] Oevering H, Paddon-Row MN, Heppener M, Oliver AM, Cotsaris E, Verthoeven JV, et al. J Am Chem Soc 1987;109:3258.
- [7] Kawamura K. In: Fouassier JP, editor. Photochemistry and UV curing: new trends, vol. XVIII. India: Research Signpost; 2006. p. 203–18.
- [8] Chatterjee S, Gottschalk P, Davis PD, Schuster GB. J Am Chem Soc 1988;110:2326.
- [9] Chatterjee S, Davis PD, Gottschalk P, Kurz ME, Sauerwein B, Yang X, et al. J Am Chem Soc 1990;112:6329.
- [10] Deligeorgiev T, Vasilev A, Tsvetkova T, Drexhage KH. Dyes Pigments 2007;75:658–63.
- [11] Deligeorgiev T, Timcheva I, Maximova V, Gadjev N, Vassilev A, Jacobsen J-P. Dyes Pigments 2004;61:79–84.
- [12] Damico R. J Org Chem 1964;29:1971–6.
- [13] Andrzejewska E, Andrzejewski M. J Polym Sci Part A Polym Chem 1998;36:665.
- [14] Brooker LGS, Keyes G, Williams W. J Am Chem Soc 1942;64:199.
- [15] Beilenson B, Hamer FM. J Chem Soc 1939:143.
- [16] Atkins PW. Physical chemistry. Oxford University Press; 1998.
- [17] Mishra A, Newkome GR, Moorefield ChN, Godinez LA. Dyes Pigments 2003;58:227–37.
- [18] Godinez LA, Patel S, Criss CM, Kaifer AE. J Phys Chem 1995;99:17449.
- [19] Rehm D, Weller A. Isr J Chem 1970;8:259.
- [20] Marcus RA. J Chem Phys A 1956;24:966.
- [21] Pączkowski J, Kucybała Z. Macromolecules 1995;28:269.
- [22] Pączkowski J, Pietrzak M, Kucybała Z. Macromolecules 1996;29:5057.